

IMPROVED ADHESION IN ELASTOMERIC LAMINATES USING ELASTOMER BLENDS

JIANAN YI,^{1*} ERIN KEANEY,¹ JINDE ZHANG,¹ CHRISTOPHER J. HANSEN,² WALTER ZUKAS,³ JOEY MEAD¹

¹PLASTICS ENGINEERING DEPARTMENT, UNIVERSITY OF MASSACHUSETTS LOWELL, LOWELL, MA 01854

²MECHANICAL ENGINEERING DEPARTMENT, UNIVERSITY OF MASSACHUSETTS LOWELL, LOWELL, MA 01854

³THE U.S. ARMY COMBAT CAPABILITIES DEVELOPMENT COMMAND SOLDIER CENTER, NATICK, MA 01760

RUBBER CHEMISTRY AND TECHNOLOGY, Vol. 95, No. 3, pp. 465–478 (2022)

ABSTRACT

Interlayer adhesion between distinct rubber compositions in elastomeric laminates has been pursued by a variety of approaches, including treating surfaces, introducing assistant chemicals, and interposing a “transition layer.” Each approach, however, may be specific to the elastomer chemistries and may not be easily transferred to other rubber composition pairs in laminates. These limitations were overcome by inserting a layer at the interface that is a blend of each of the elastomer compositions of the adjacent layers and that increases the interfacial adhesion strength of the resultant laminates. This approach was demonstrated using three elastomer systems: fluoroelastomer (FKM), acrylonitrile–butadiene rubber (NBR), and isobutylene–isoprene rubber (IIR). The adhesion in the three-layer laminate (FKM/NBR/IIR) was improved with the addition of an FKM–NBR blend layer between the FKM and NBR layers and the addition of an NBR–IIR blend layer between the NBR and IIR layers. The five-layer laminate (FKM/[FKM–NBR blend]/NBR/[NBR–IIR blend]/IIR) was also fabricated. Interfacial adhesion was evaluated using the T-peel test according to ASTM D1876, which showed that the blends provided improved adhesion. Scanning electron microscope images were used to study the interface region. The proposed idea offers a general approach to improve interfacial strength that is widely applicable to other multilayer elastomer laminates. [doi:10.5254/rct.22.78968]

INTRODUCTION

Military personnel, industrial workers, and emergency responders commonly face toxic threats such as chemical, radiologic, physical, electrical, mechanical, or other workplace hazards.^{1,2} The Human Rights Council estimates that, globally, one worker dies every 15 s from toxic exposure at work, and more than 2,780,000 employees die worldwide from risky work conditions every year.³ Chemical protective clothing (CPC) plays a critical role in protecting personnel by shielding or isolating workers from exposure to solid, liquid, and gaseous hazards by blocking the penetration and permeation of the hazardous substance.

CPC clothing is fabricated from a range of polymeric materials, including both thermoplastics (e.g., polyethylene, chlorinated polyethylene, polyvinyl alcohol, polyvinyl chloride, polytetrafluoroethylene) and crosslinked elastomers (e.g., butyl rubber, chlorinated butyl rubber, nitrile rubber, polyurethane rubber, fluoroelastomer).⁴ These barrier materials, which may be combined with absorbents such as activated ASZM–TEDA carbon (a grade of carbon), absorb the chemicals to slow or prevent permeation.⁵

The main drawback of both single-layer thermoplastic and crosslinked elastomer CPC is that their chemical protection is limited to a subset of toxic industrial chemicals (TICs) and other chemical agents. To improve the chemical resistance and physical properties of products preferred for demanding working conditions, manufacturers often create multilayer structure laminates for CPC materials that combine the advantages of each individual layer's properties.^{4,6}

Combinations of one thermoplastic with a layer of textile or coating that could obtain satisfactory chemical resistance materials have been disclosed. For example, Effenberger et al.⁷ coated fluoropolymer or polyphenylene sulfide on textiles such as woven fiberglass; Smith⁸ co-extruded a three-layer structure, polyethylene–ethylene vinyl alcohol–polyethylene, as a barrier

*Corresponding author. Ph: (+49) 0174-6071-896; email: Jianan_Yi@student.uml.edu

layer and then laid them on a web of PYROLON (about 60% wood fiber and about 40% polyester) to fabricate garments; one layer of elastomeric blends composing of 50% vinylidene fluoride and 50% hexafluoropropene was coated on polytetrafluoroethylene fabric, resulting in a flexible garment.⁹ For multilayer elastomers, fluoroelastomer and nitrile elastomer are often combined to improve the fuel resistance for hose applications.^{10,11}

Elastomeric barrier materials are attractive for CPC garments because of their excellent chemical resistance and intrinsic flexibility/elasticity. Fluoroelastomers (e.g., FKM) have excellent resistance to a wide range of chemicals, such as fuels, petroleum oils, and most mineral acids. However, FKM is expensive^{12,13} and is thus often combined with other elastomers in the form blends or laminates^{14–16} to reduce the cost. Other elastomers such as acrylonitrile–butadiene rubber (NBR) and isobutylene–isoprene rubber (IIR) can resist chemicals such as ethers, esters, ketones, alkalis, and amines, against which FKM has relatively poor resistance.¹⁷ Moreover, IIR also has excellent gas impermeability, which can result in an airtight CPC garment that meets the most protective level (level A) according to the Occupational Safety and Health Administration and resists some gaseous chemicals.^{18–20}

Accordingly, a multilayer laminate comprising FKM, NBR, and IIR is expected to satisfy the chemical barrier material requirements in terms of chemical resistance, flexibility, elasticity, gas impermeability, and enhanced mechanical strength for exposure to a broad range of chemical agents.

In a multilayer laminate, the interlayer adhesion strength is essential to the effectiveness of multilayer CPC clothing, because chemical contact can weaken the adhesion, resulting in delamination.^{21,22} The adhesion between elastomer layers, however, is a challenge because of the different chemical and physical properties of the rubber materials. Increasing the adhesion of rubber to different substrates has been explored through approaches such as surface treatment and adhesion promoters, which are detailed in two comprehensive reviews given by Bhowmick and Rezaeian.^{23,24}

One common approach is to apply a surface modification to one of the surfaces, aiming to increase the surface energy, enhance wetting, and improve the adhesion. Examples include the surface halogenation of natural rubber thermoplastic elastomers, which improved their adhesion to acrylic tapes²⁵; the surface modification of ethylene propylene diene monomer (EPDM) rubber with gamma irradiation, which resulted in an increase in the adhesion strength between EPDM and natural rubber (NR)²⁶; the corona discharge treatment of chlorobutyl rubber–NR blend, which promoted its adhesion to an elastomeric polyurethane coating²⁷; and the oxygen plasma treatment of an NBR-cured sheet, which resulted in higher adhesion to a coated nylon layer.²⁸

The incorporation of adhesion promoters and compatibilizers through compounding is another way to improve the adhesion. Adding proper tackifiers, such as coumarone indene resin, into elastomer-based pressure-sensitive adhesives achieved better wettability and tack between the adherends.^{29–31} NR filled with hydrophilic silicon dioxide powder strongly adhered to a heat-assisted plasma-treated polytetrafluoroethylene surface.³² Ethylene-co-vinyl acetate was used as a compatibilizer to improve NR–NBR blend properties attributed to the increased interfacial adhesion in the blends, as did NR used as a compatibilizer in a styrene–butadiene rubber (SBR)–NBR blend.^{33,34} Improving the bonding between FKM and NBR was studied by compounding amine-terminated acrylonitrile butadiene (ATBN), epoxy resins, or phosphonium salt into the formulations.^{15,16,35,36} NBR and IIR adhesion was investigated by adding succinic–anhydride-terminated polyisobutylene into the IIR formulation and adding ATBN into the NBR formulation.³⁷

A third way to improve the adhesion between two layers with distinct compositions is to interpose a “transition layer,” which acts like a coupling agent, between the two adjacent layers.

This transition layer can be realized by applying primers,³⁸ layers containing graft polymers,^{39,40} tie layers,⁴¹ or directly applying adhesive.⁴²

The adhesion approaches discussed above successfully improve the interfacial bonding strength between different materials. The challenge resides with the lack of general transferability to a broad range of material systems. Although there are numerous accounts of using graft and block copolymers to act as interfacial bridges to reduce the interfacial tension, improve interfacial adhesion, and therefore modify the morphology of the blends,^{43–48} there has been little reported on the use of rubber blends to improve the bonding of two different rubber laminates. For example, a blend of rubber A and rubber B could be considered as an interlayer between a layer of pure rubber A and pure rubber B. In this case, improved adhesion is expected because the middle layer contains the same components as the individual layers do. If proven, this general approach is more feasible and transferrable because it leverages self-adhesion, an intrinsic property of elastomers, which can exceed the adhesion strength of elastomers to a different substrate.^{49–52} Moreover, no extra polymers or chemicals are introduced into the elastomer matrices, thereby avoiding any potential detrimental effects on vulcanization or properties.

The present work investigates the use of rubber blends to adhere chemically distinct rubber layers to form a multilayer laminate. A three-layer elastomer laminate consisting of FKM, NBR, and IIR layers was selected to demonstrate this conceptual approach. The resulting multilayer laminate consisted of three primary layers (FKM, NBR, and IIR) and two rubber blend interlayers, that is, FKM–NBR blend and NBR–IIR blend. The morphology at the interface was characterized by microscopy. The adhesion of the adjacent layers in a two-layer cured laminates was quantified by the T-peel test.

EXPERIMENTAL

MATERIALS

The FKM used for this study was Viton™ grade A401C (Chemours Company, Wilmington, DE, USA) and selected as the outer layer for the laminate. Its specific gravity is 1.82 with a Mooney viscosity ML (1+10) at 121 °C of 42. The NBR used was Nipol® 1051 with a 41% acrylonitrile content (ZEON Chemicals L.P., Louisville, KY, USA) used as the middle layer for the laminate. Its specific gravity is 1.00 with a Mooney viscosity MS (1+4) at 100 °C ranging from 63 to 78. The IIR used as the other outer layer was Exxon™ Butyl 268S with a specific gravity of 0.92 and a Mooney viscosity (ML 1+8) at 125 °C of 51. The cure systems for the compounded formulations included zinc oxide (ZnO; grade ZOCO 102 USP, Zochem LLC, Dickson, TN, USA) with a surface area of 8–9 m²/g, stearic acid (SA; purified grade, Sigma Aldrich, St. Louis, MO, USA); 1,3-diphenylguanidine (DPG; 97% purity, Sigma-Aldrich); calcium hydroxide (Ca(OH)₂; >96%, Sigma-Aldrich); high-activity magnesium oxide (MgO; STAR MAG U, HB Chemical, Twinsburg, OH, USA); and sulfur (S; S 104, Harwick Standard Distribution, Pico Rivera, CA, USA).

SAMPLE PREPARATION AND CHARACTERIZATION

Mastication. — A lab-use two-roll mill (C.W. Brabender Instruments, Inc., Hackensack, NJ, USA) was used to masticate the elastomers. For mastication, a gap of 0.001–0.002 inch, a speed of 6 rpm, and a set temperature of 40 °C were used. FKM and IIR were masticated for 2 to 3 min and then used for subsequent operations. NBR was masticated for 10 min and cut into smaller pieces. During the mastication, the material temperatures reached up to 45 °C.

Mixing. — Mixing of the rubber formulation was performed using an internal mixer (Plasti-Corder, C.W. Brabender Instruments, Inc.) with a set temperature of 80 °C. FKM 100 parts per hundred rubber (phr) was compounded by being fed into the mixing bowl for 2 min with a rotor speed of 20 rpm. After 2 min, the speed was increased to 60 rpm, and 3 phr MgO and 6 phr Ca(OH)₂ were added. Another 5 min were given to fully mix all ingredients. Similarly, 100 phr of NBR was fed into the mixing bowl for 2 min with a rotor speed of 20 rpm. The speed was then elevated to 60 rpm, and 3 phr ZnO and 1 phr SA were added and mixed with the rubber for 1.5 min. Next, 3 phr DPG was added and mixed for another 1.5 min. Finally, 1 phr sulfur was added, and the full compound was mixed for a final 5 min. The compounding of IIR (formulation: 100 phr IIR, 3 phr ZnO, 1 phr SA, 3 phr DPG, 1 phr S) was performed in exactly the same manner as for the NBR.

Rubber blends were created from the above compounds. The specific gravity of FKM is almost twice that of NBR, whereas NBR and IIR have almost the same specific gravity. To ensure a commensurate volumetric portion in the blends, the weight ratio of FKM to NBR was 2:1, and the weight ratio of NBR to IIR was 1:1. The mixing process involved feeding the proper amounts of each rubber into the two-roll mill to make a blend, with a speed of 6 rpm at 40 °C for 10–15 min (gap: 0.001–0.002 inch). The resultant rubber sheet was fed into the internal mixer to eliminate potential trapped air (temperature: 80 °C, rotor speed: 20 rpm, time: 2–3 min). The resulting blends will be referred to as FKM-NBR blend and NBR-IIR blend.

Rubber Curing Test. — A rubber process analyzer (RPA2000, Alpha Technologies, Hudson, OH, USA) was used to study the cure behavior of the rubber compound or blend according to ASTM D2084-17. The preheating time was 30 s at 160 °C, and the specimen was tested at the same temperature using a frequency of 100 CPM (number of cycles per minute, or 1.67 Hz) and oscillation degree of 1°. The scorch time (t_s 1), optimum cure time (t'_{90}), and cure rate index (CRI) were calculated based on the raw data.

Laminate Fabrication. — The compounds and blends were preshaped individually in a mold using a hydraulic compression molding machine (Wabash) at 100 °C for 5 min under a force of 1.97×10^5 N to make circular specimens having an approximate thickness of 3.5 mm and a diameter of 7 cm. Then, a pair of preshaped specimens were assembled together with a piece of thin polyester film (130 mm \times 130 mm \times 0.03 mm) inserted between the two layers on one edge, which was intended to generate two free “tabs” for the T-peel test. Next, these two layers were placed between two preheated aluminum plates, where at least two smaller metal shims were inserted to control the thickness of the final laminates. Before applying a force of 1.97×10^5 N to the plates, the two layers were preheated for 30–40 s, and then the two plates were closed gradually. The cure was conducted at 160 °C for 25 min, and the result was a two-layer laminate with an overall thickness of approximately 1.7 mm. The edge of the laminates contained interlaminar air voids; to avoid the effects of such voids, the edge sections were trimmed before further testing. The remaining parts were cut into strips with a width of 2.5 cm.

Interface Layer Study. — A five-layer laminate, FKM/(FKM-NBR blend)/NBR/(NBR-IIR blend)/IIR, was made in same manner, with a final thickness of about 5.3 mm. The four interfaces in the five-layer laminates were characterized by scanning electron microscopy (SEM; JSM 7401F, JEOL) at 2.0 kV. The cross-section of the five-layer laminate was viewed using a Zeiss Stereo V20 microscope.

T-Peel Test. — The adhesion strength of the laminates was evaluated using the T-peel test according to ASTM D1876. A universal testing machine (Instron model 4444, Instron Corporation, Norwood, MA, USA) was used to load the 2.5 cm width strips at a speed of 254 mm/min. A minimum of three strips of each laminate type were tested, and the average T-peel force was reported.

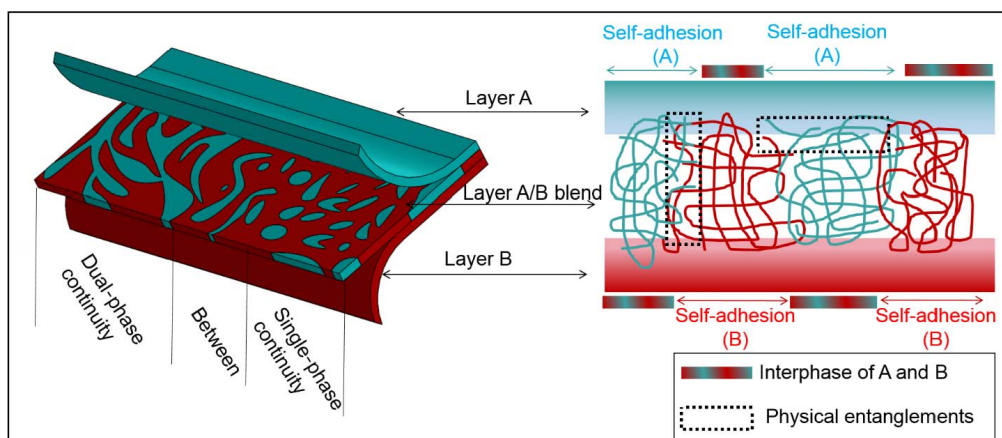


FIG. 1. — Schematic of the rubber blends method for improving the interfacial adhesion in a multilayer laminate. A and B refer to any polymer materials (either thermoplastics or thermosets). (Left) Possible single- and dual-phase morphologies of the blend layers. (Right) Cross section of the multilayer laminate, in which the middle blends layer adheres to both sides of the interface.

RESULTS AND DISCUSSION

RATIONALE

Self-adhesion is an intrinsic property of both elastomers and thermoplastics. The improved adhesion caused by the rubber blends is mainly attributed to the self-adhesion of the component present in the neat layer and the blends layer. Because the rubber blends method harnesses this self-adhesion behavior, it can be generally applied to a broad array of other materials sets, without resorting to polymer synthesis.

A schematic of how the rubber blends improve the adhesion between layers within a laminate is shown in Figure 1. In the case of excellent compatibility between materials, the polymer chains may adequately interdiffuse, leading to entanglement of the chains and strong adhesion; in these cases, a blend layer is probably not necessary. In the case of weak adhesion or poor compatibility, such as in the case of FKM/NBR and NBR/IIR, an alternative strategy is required; a blend layer can be interposed between the layers to improve adhesion, regardless of the compatibility of polymer A and B. In the case of a miscible blend, there will be a single phase, but for most high-molecular-weight polymers, the morphology depends on the relative compatibility between the two polymers.^{53,54}

Regions in Figure 1 where the same color is present on both sides of the interface show self-adhesion between polymer chains of polymer A or B with itself. By contrast, regions with different colors at the interface indicate the adhesion between polymer A and B. In these regions, the adhesion is driven by both chemical interactions (e.g., Van der Waals), chemical bonds (e.g., crosslinking), and physical entanglements among polymer chains or phases. In the case of incompatible materials, the adhesion between them will be weak but can be enhanced by a co-continuous morphology of the two materials or crosslinking reactions between the two polymers during curing. Interposing a blend layer can increase the adhesion force by means of creating this morphology to improve the adhesion between two materials that do not bond well. Because two polymers are considered immiscible when the solubility parameter difference ($\Delta\delta$) is greater than 0.5,⁵⁵ the cases of FKM, NBR, and IIR discussed in this article would benefit from this approach (solubility parameter δ : FKM 13.5–17.8 [MPa]^{1/2}; NBR 18.3–20.3 [MPa]^{1/2}; IIR 15.8–16.5 [MPa]^{1/2}).⁵⁶

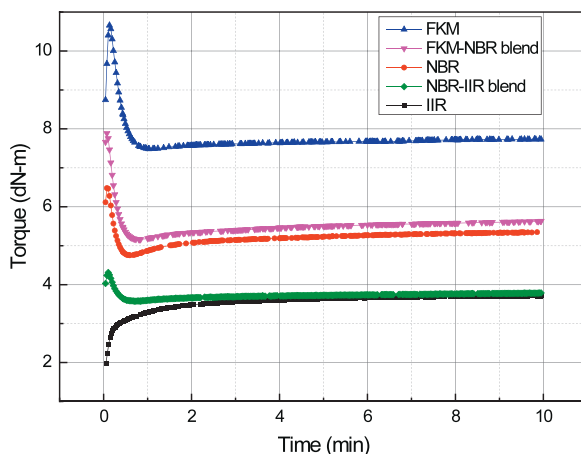


FIG. 2. — Torque vs time for RPA testing of FKM, FKM–NBR blend, NBR, NBR–IIR blend, and IIR at 100 °C for 10 min.

RUBBER CURING TEST

Bhowmick and Gent⁴⁹ studied the effect of partial crosslinking time (t_1 , the time before assembling two layers together) on the self-adhesion of SBR and neoprene rubber when the total cure time was ($t_1 + t_2$; where t_2 is the second cure time) and found that a longer t_1 would decrease the self-adhesion strength. It is therefore important to ensure the rubber layers are crosslinked as little as possible before making intimate contact. Accordingly, it is necessary to examine whether crosslinking occurs in the preshaping step (occurring at 100 °C). Figure 2 shows the RPA tests of the three primary elastomer compounds and the two blends at 100 °C for 10 min.

For rubber curing, the viscosity and corresponding torque exerted on the rotors will decrease as the compounding is heated. The torque will decrease and then increase as the rubber begins the curing. As the curing proceeds, the torque rises and then levels off with full cure. The curve may also reach a plateau, continue to rise (marching), or become lower (reversion) with time, which depends on the specific rubber formulation.⁵⁷ The FKM and NBR–IIR blend had almost no change in torque (<0.5 dN-m) after the minimum torque occurred. The FKM–NBR blend and NBR had a slight increase in torque (~ 0.5 dN-m) and thus negligible curing. The IIR showed a slight increase in torque due to the flow of IIR to fully fill the diaphragm die of the RPA, but there was no significant increase in torque due to curing. Overall, Figure 2 indicates no significant crosslinking would have occurred in any of the rubber compounds and blends at 100 °C in the preshaping step at 100 °C (5 min), assuring good adhesion in the lamination step.

The cure dynamics of the elastomers at 160 °C are shown in Figure 3. From this graph, the cure parameters, including t_{ML} (the time at which the torque is minimum, M_L), t_{MH} (the time at which the torque is maximum, M_H), t_{s1} (the time to 1 dN-m rise above M_L , 1° oscillation amplitude), cure time (t'_{50} and t'_{90} , the time to 50% and 90% of the torque increase, respectively), and cure rate index ($CRI = 100/t'_{90} - t_{s1}$) were calculated. These parameters are summarized in Table I.

At t_{ML} , these rubber compounds and blends had different M_L ; thus, different viscosities or/and hardness might ultimately affect the thickness of the individual layers in the compression molded laminates. FKM had the highest M_H , followed by NBR, and IIR had with the lowest M_H . The torque of the FKM–NBR blend was not between that of FKM and NBR but rather much lower than both. This lower value is caused by the bisphenol AF crosslinking agent for FKM, which acts to inhibit the radical vulcanization of the diene rubber (NBR); in addition, the radical vulcanization could further cause the decomposition of bisphenol AF, which would adversely affect the cure of

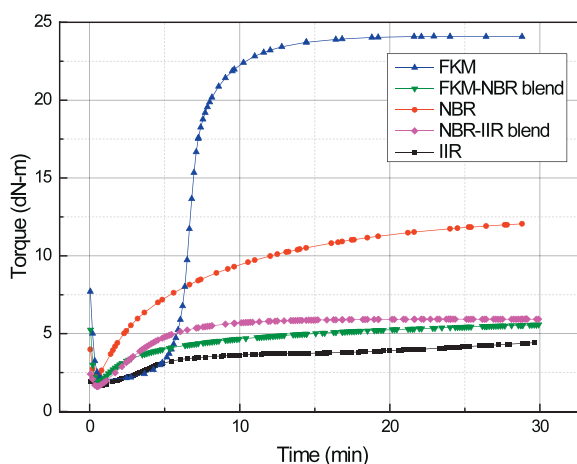


FIG. 3. — Torque vs time cure behavior of FKM, NBR, IIR, FKM–NBR blend, and NBR–IIR blend at 160 °C.

FKM.^{58,59} The torque of the NBR–IIR blend was intermediate to that of NBR and IIR but substantially lower than that of NBR. From Table I, we can note that although the t_s1 , $t'90$, and CRI of these rubber compounds and their blends are different, they all undergo their curing reactions within approximately the range from 3 to 10 min and achieve complete cure by about 10 min (Figure 3). This overlap in cure times ensured the potential for good adhesion and potential crosslinking between different rubbers to be generated in the laminate, as the adhesion of an uncured rubber to a fully cured rubber might be poor.

T-PEEL TEST

In the T-peel tests, cohesive failure corresponds to failure that occurs in the layers, rather than in the interfacial region; this type of failure typically suggests the adhesion strength is greater than the tensile strength of either layer. By contrast, apparent interfacial failure means the failure occurred at the interface between the two layers, indicating that the tensile strength of either layer in the laminate is greater than the adhesion strength. Figure 4 shows representative load-extension curves from the T-peel tests for the six pairs of laminates. For all laminates that show adhesion, the loading

TABLE I
CURE PARAMETERS OF ELASTOMER COMPOUNDS

| Term | Minimum torque | | Maximum torque | | Scorch time | Cure time | | | Cure rate index |
|---------------|----------------|----------|----------------|----------|-------------|-----------|--------|-------------------|-----------------|
| | M_L | t_{ML} | M_H | t_{MH} | | t_s1 | $t'50$ | $t'90$ | |
| Symbol | M_L | t_{ML} | M_H | t_{MH} | t_s1 | $t'50$ | $t'90$ | CRI | |
| Unit | dN-m | min | dN-m | min | min | min | min | min^{-1} | |
| IIR | 1.79 | 0.7 | 4.4 | 29.6 | 3.8 | 4.9 | 26.3 | 4.4 | |
| NBR | 2.2 | 0.4 | 12.16 | 28.8 | 1.4 | 4.8 | 18.5 | 5.9 | |
| FKM | 2.1 | 1.1 | 24.1 | 22.9 | 4.7 | 6.8 | 9.5 | 20.8 | |
| FKM–NBR blend | 1.9 | 0.6 | 5.6 | 29.9 | 1.9 | 4.0 | 20.2 | 5.5 | |
| NBR–IIR blend | 1.6 | 0.6 | 6.0 | 29.1 | 1.7 | 3.4 | 8.1 | 15.6 | |

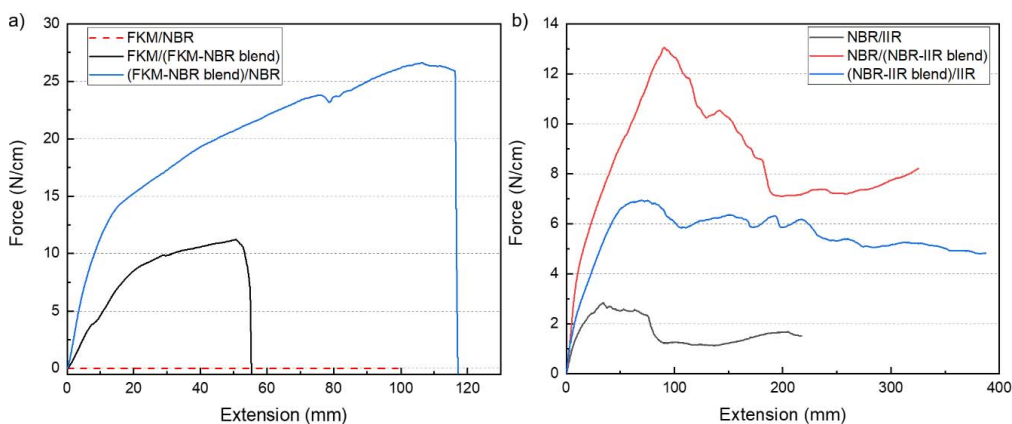


FIG. 4. — Representative load-extension results of the T-peel test for the six pairs of laminates: (a) load-extension curves for combinations of FKM and NBR, laminates 1, 2, and 3; (b) load-extension curves for combinations of NBR and IIR, laminates 4, 5, and 6.

force experiences a maximal peak as the extension increases, followed by fluctuations at a relatively lower level.⁶⁰ For the laminates containing FKM and NBR, the breaking point can be clearly observed in the corresponding load-extension curve (black and blue curves in Figure 4a). For the NBR- and IIR-containing laminates, the test ends at the maximum extension of the laminates in the T-peel geometry without observing a fracture point in either layer, as shown in Figure 4b.

The T-peel test results are summarized in Table II. The first laminate tested was a combination of the FKM and NBR primary elastomers. Without any bridging layers or surface treatments between FKM and NBR, the layers delaminated when opening the molds during the laminate fabrication and no adhesive force was measured (indicated by the red dashed line in Figure 4a). By contrast, laminate FKM/(FKM-NBR blend) and laminate (FKM-NBR blend)/NBR demonstrated robust adhesion; rather than apparent interfacial failure, FKM cohesive failure and FKM-NBR blend cohesive failure were observed, respectively, in which case the exact interfacial adhesion was unknown but should be higher than the tested cohesive strength (i.e., the breaking point >10 N/cm and >26 N/cm in Figure 4a). From these results, it can be inferred that FKM and NBR can be tightly bonded using an FKM–NBR blend layer at their interface.

Similarly, the adhesion between the NBR and IIR layers was poor, with an average adhesive strength of only 1.6 N/cm. The adhesion strength in laminate NBR/(NBR-IIR blend) was 9.2 N/cm and in laminate (NBR-IIR blend)/IIR was 5.6 N/cm, representing a fivefold and threefold increase, respectively, in the adhesion strength relative to an NBR/IIR laminate without any treatments.

TABLE II
ADHESION FORCE FROM T-PEEL TESTING FOR TWO-LAYER LAMINATE COMBINATIONS

| Laminate No. | Two-Layer Laminate | Adhesion, N/cm | Failure type |
|--------------|---------------------|----------------|------------------------|
| 1 | FKM/NBR | 0 | No adhesion |
| 2 | FKM/(FKM–NBR blend) | >10 | FKM cohesive |
| 3 | (FKM–NBR blend)/NBR | >26 | FKM–NBR blend cohesive |
| 4 | NBR/IIR | 1.6 | Apparent interfacial |
| 5 | NBR/(NBR–IIR blend) | 9.2 | Apparent interfacial |
| 6 | (NBR–IIR blend)/IIR | 5.6 | Apparent interfacial |

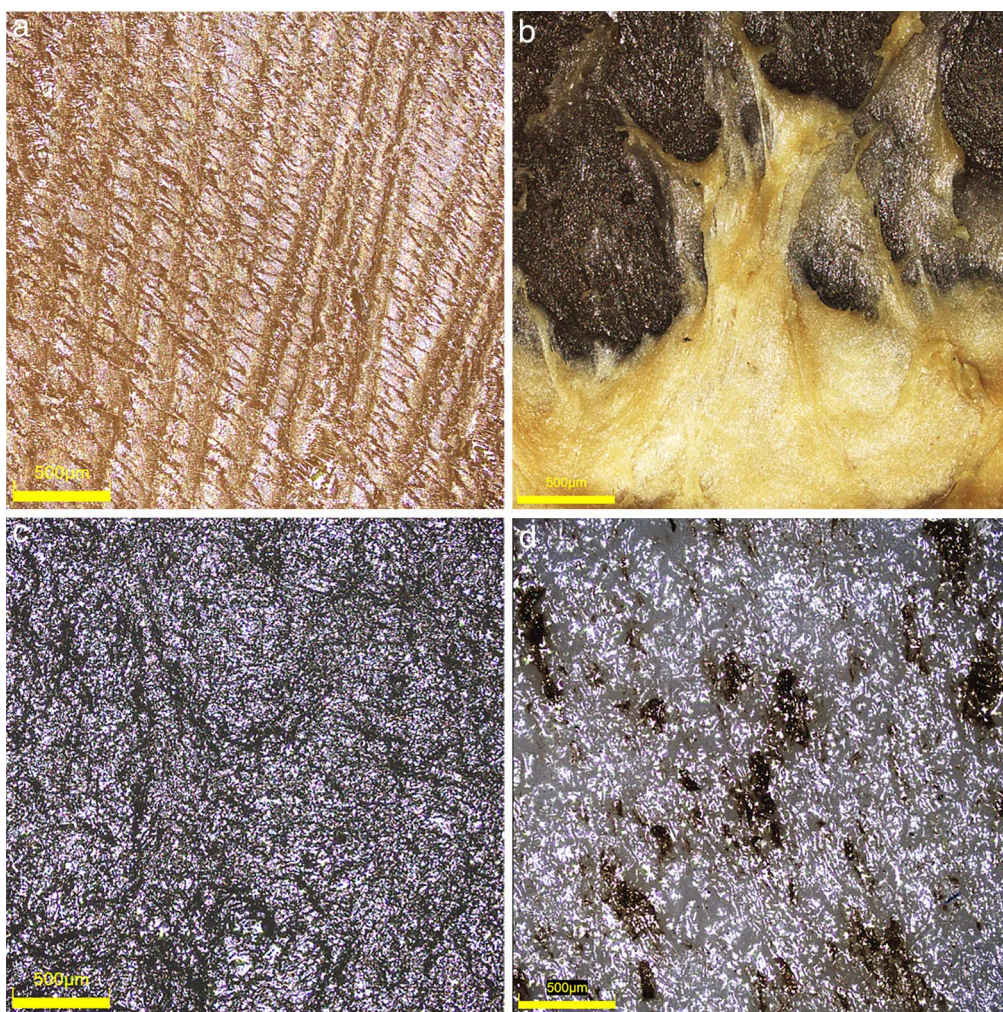


FIG. 5. — Optical images of laminate (FKM–NBR blend)/NBR and laminate (NBR–IIR blend)/IIR after T-peel test: (a) FKM–NBR blend layer, (b) NBR layer, (c) NBR–IIR blend layer, and (d) IIR layer.

Thus, NBR and IIR are able to be bonded with improved adhesion by placing a blend layer between the individual elastomer layers. The more modest improvement in adhesion compared with that seen for the FKM–NBR system might be due to the large difference in polarity and the poor compatibility between NBR and IIR.⁶¹ The adhesion strength might be further improved through optimizing the blend performance by precurcuring IIR⁶¹ or by introducing compatibilizers such as bromobutyl rubber⁵⁴ or chlorinated polyethylene.⁶²

Two example laminates—the (FKM–NBR blend)/NBR and the (NBR–IIR blend)/IIR laminates—are shown in Figure 5 to help explain the function of the blend layer with respect to improving the adhesion. The (FKM–NBR blend)/NBR laminate is shown in Figure 5a,b. In Figure 5a, the surface of the FKM–NBR blend layer after the T-peel test shows a coarse microscale texture. This texturing may be indicative of better adhesion to the NBR layer from an increased contact surface area and potential migration of the polymer chains across the interface. This texturing is more clearly seen in the residues of the FKM–NBR blend (yellow) in Figure 5b, which are still

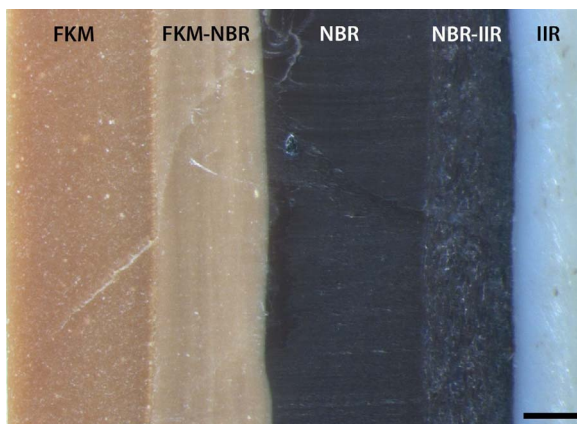


FIG. 6. — Optical cross-section view of the five-layer laminate. From left to right, the layers are FKM, FKM–NBR blend, NBR, NBR–IIR blend, and IIR. Scale bar is 500 μm . The total laminate thickness is 5.3 mm.

adhered to the NBR layer after the blend layer fractured in the test. For the laminate (NBR–IIR blend)/IIR after the T-peel test, there is less coarse texturing on the NBR–IIR blend layer (Figure 5c) but still some blend residue (brown spots) remaining on the IIR layer (white). This reduced interaction is reflected in the T-peel test results (the NBR–IIR blend layer has lower improvement in adhesion between the NBR and IIR as compared with the FKM–NBR blend layer promoting adhesion increase between FKM and NBR).

INTERFACE LAYER STUDY

The blend layer approach was used to create a five-layer laminate. A cross-section view of the five-layer laminate is shown in Figure 6. The five layers appear visibly well bonded. The variation in layer thicknesses is attributed to the different hardness and flowability of these rubber compounds and blends during the laminate compression at 160 °C. The torque values (shown in Figure 3) range from approximately 5 to 25 dN-m, demonstrating the broad range of the physical properties.

More detailed images of the interfaces were characterized by SEM (Figures 7 and 8). The interface between the FKM–NBR blend and either FKM or NBR is visible in Figure 7a,c. Under greater magnification (Figure 7b,d), the blend appears to be uniformly compounded, enabling strong adhesion in the laminate FKM/(FKM–NBR blend) and laminate (FKM–NBR blend)/NBR. The NBR in the FKM–NBR blend is able to adhere strongly to the neat NBR layer (NBR self-adhesion), and the FKM in the blend can likewise adhere to the neat FKM layer (FKM self-adhesion).

As compared with the more homogeneous structure observed in the FKM–NBR blends, the NBR and IIR blends show greater heterogeneity. In Figure 8, the individual phases of NBR and IIR are visible in their blends, with the lighter color phase being IIR and the darker phase being NBR. The neat NBR layer bonds with the NBR phase in the NBR–IIR blend (NBR self-adhesion), and the neat IIR layer is also bonded with the IIR phase in the NBR–IIR blend (IIR self-adhesion), which improved the adhesion between NBR and IIR by the same mechanism as described for the NBR and FKM bonding. The greater heterogeneity of the blend structure indicates that the NBR and IIR have lower chemical compatibility with each other compared with the NBR and FKM. This lower compatibility corresponds to the lower interfacial adhesion strength observed for the NBR–IIR blend system.

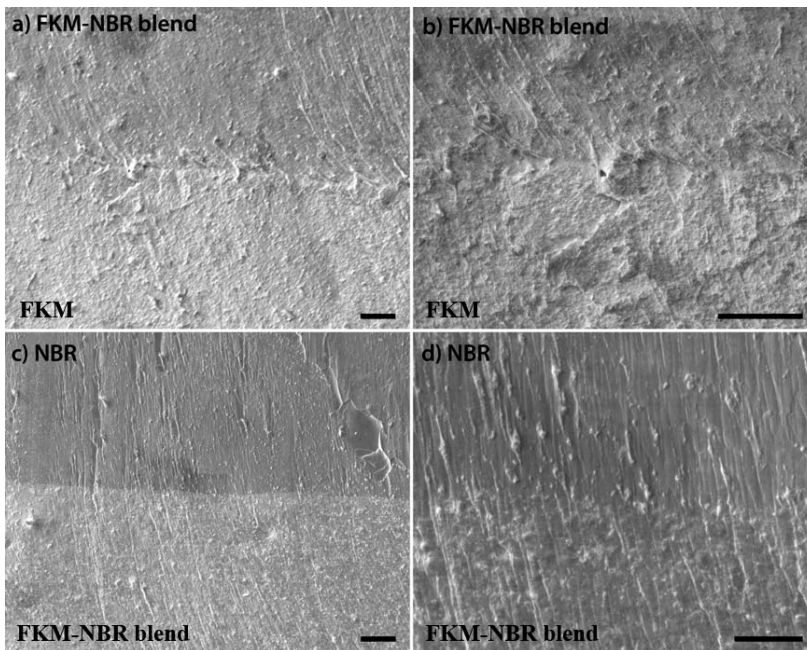


FIG. 7. — SEM images of the FKM, NBR, and FKM-NBR blend interfaces. (a, b) Interface between FKM and FKM-NBR blend layers. Scale bars 100 μm . (c, d) Interface between FKM-NBR blend and NBR layers. Scale bars 100 and 50 μm , respectively.

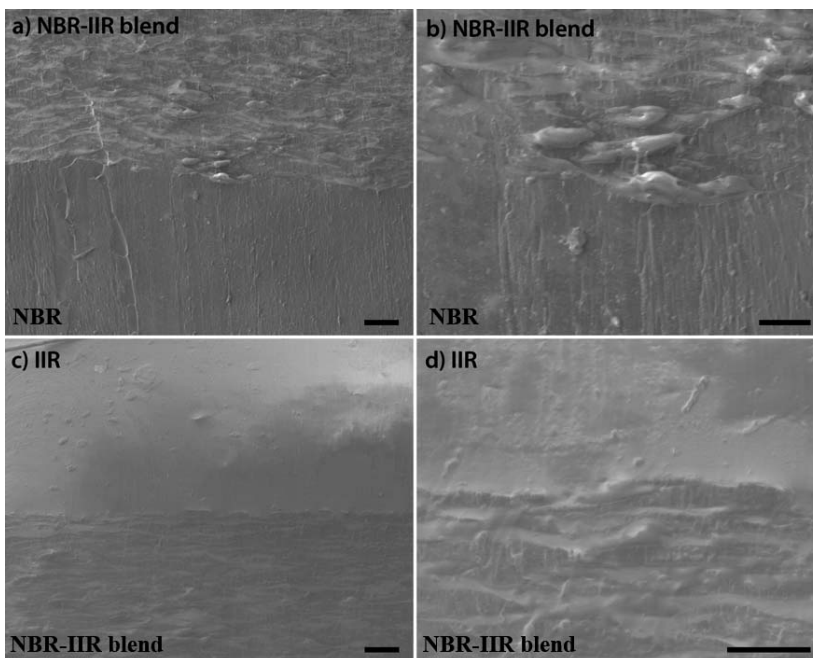


FIG. 8. — SEM images of the NBR, IIR, and NBR-IIR blend interfaces. (a, b) Interface between NBR and NBR-IIR blend layers. Scale bars 100 and 50 μm , respectively. (c, d) Interface between NBR-IIR blend and IIR layers. Scale bars 100 and 50 μm , respectively.

CONCLUSIONS

This work studied the use of rubber blends to improve the adhesion between elastomer materials with poor adhesion. The specific material systems studied were FKM–NBR and NBR–IIR, whose neat compositions exhibit poor interfacial adhesion strength. The RPA results showed that these three elastomer compounds and their blends (FKM–NBR blend, NBR–IIR blend) have overlapping curing times, which enable rubber self-adhesion during curing between the pure elastomer and the component in the blend. The overlapping cure times enabled the creation of co-vulcanized blends to bond laminates with good adhesion strength. After introducing the blend layers, the adhesion between FKM and NBR was improved from 0 N/cm to greater than 10 N/cm, and the adhesion between NBR and IIR was improved from 1.6 N/cm to greater than 5.6 N/cm. A five-layer laminate was manufactured, and SEM images indicated robust adhesion between the layers. This method for improving adhesion in a multilayer laminate is easily transferable to other material pairs in laminates and is a relatively low-cost approach requiring no additional additives.

ACKNOWLEDGEMENTS

This work was funded by the U.S. Army Combat Capabilities Development Command Soldier Center (Natick, MA) under contract number W911QY-17-2-0004. The authors thank Vanderbilt Chemicals, LLC for providing butyl rubber, Zochem LLC for providing ZnO, and HB Chemical for providing MgO.

REFERENCES

- ¹J. L. Arnold, S. White, F. Talavera, and R. J. Roberge, *Emedicinehealth* (2018).
- ²Chairman of the Joint Chiefs of Staff, *Operations in Chemical, Biological, Radiological, and Nuclear Environments*. Joint Publication 3-11 (2018).
- ³Human Rights Council (United Nations), “Report of the Special Rapporteur on the Implications for Human Rights of the Environmentally Sound Management and Disposal of Hazardous Substances and Wastes,” 2018, <https://Digitallibrary.Un.Org/Record/1654299?Ln=en>. Accessed May 1, 2022.
- ⁴K. Forsberg and L. H. Keith, *Chemical Protective Clothing: Permeation and Degradation Compendium*, CRC Press, New York, 1995.
- ⁵R. W. Morrison, “Title,” 20013. <https://Www.Hsdl.Org/?Abstract&did=453463>. Accessed May 1, 2022.
- ⁶E. V. Wely, *Ind. Health* **55**, 485 (2017).
- ⁷J. A. Effenberger, R. C. Ribbans III, and F. M. Keese (to Chemical Fabrics Corporation), U.S. Patent 4,610,918, September 9, 1986.
- ⁸W. Smith Novis (to Lakeland Industries, Inc.), U.S. Patent 5,491,022, February 13, 1993.
- ⁹H. I. Snyder and E. E. Plumb, U.S. Patent No. 3,547,765, December 15, 1970.
- ¹⁰M. Ichikawa and T. Okita (to Toyoda Gosei Co., Ltd.), U.S. Patent No. 5,356,681, October 18, 1994.
- ¹¹S. Kanbe, M. Kondo, and M. Nishimura (to Tokai Rubber Industries, Ltd.), U.S. Patent No. 6,340,511 B1, January 22, 2002.
- ¹²A. Ciesielski, *An Introduction to Rubber Technology*, Rapra Technology Limited, Shawbury, 1999.
- ¹³J. G. Drobny, *Fluoroelastomers Handbook*, William Andrew, Cambridge, MA, 2016.
- ¹⁴Y. Tagelsir, S. Li, X. Lv, S. Wang, S. Wang, and Z. Osman, *Mater. Res. Express* **5**, 015313 (2018).
- ¹⁵T. Nakagawa and O. Sugimoto (to Nippon Zeon Co., Ltd.), U.S. Patent 4,828,923, May 9, 1989.
- ¹⁶M. Oyama and K. Nakajima (to Nippon Zeon Co., Ltd.), U.S. Patent 5,855,976, January 5, 1999.
- ¹⁷Mykin-Inc, *Chemical-Resistance-Chart*. <http://Mykin.Com/Rubber-Chemical-Resistance-Chart>. Accessed May 1, 2022.

- ¹⁸J. P. Haworth and F. P. Baldwin, *Ind. Eng. Chem.* **24**, 1301 (1942).
- ¹⁹S. Takahashi, H. A. Goldberg, C. A. Feeney, D. P. Karim, M. Farrell, K. O'Leary, and D. R. Paul, *Polymer (Guildf)*, **47**, 3083 (2006).
- ²⁰National Environmental Inc., "Trainers Overview of HAZMAT Protection Levels," <https://www.natlenvtrainers.com/Blog/Article/Hazmat-Protection-Levels>. Accessed May 1, 2022.
- ²¹D. H. Anna, *Chemical Protective Clothing*, 2nd ed., American Industrial Hygiene Association, Fairfax, VA, 2003.
- ²²A. Flepp and M. Hoffmann (to EMS-Chemie AG), U.S. Patent 6,555,243 B2, April 29, 2003.
- ²³K. D. Kumar, M. S. Satyanarayana, G. C. Basak, and A. K. Bhowmick, *Progress in Adhesion and Adhesives*, Scrivener Publishing, Beverly, MA, 2019.
- ²⁴I. Rezaeian, P. Zahedi, and A. Rezaeian, *J. Adhes. Sci. Technol.* **26**, 721 (2012).
- ²⁵M. D. Ellul and D. R. Hazelton, *RUBBER CHEM. TECHNOL.* **67**, 582 (1994).
- ²⁶G. C. Basak, A. Bandyopadhyay, Y. K. Bharadwaj, S. Sabharwal, and A. K. Bhowmick, *J. Adhes.* **86**, 306 (2010).
- ²⁷D. F. Lawson, *RUBBER CHEM. TECHNOL.* **60**, 102 (1987).
- ²⁸S. Saitoh, M. Yoshikawa, and K. Naito, *Thin Solid Films* **316**, 165 (1998).
- ²⁹B. T. Poh and C. H. Lim, *J. Elastomers Plast.* **46**, 187 (2012).
- ³⁰B. T. Poh and A. T. Yong, *J. Macromol. Sci.* **46**, 97 (2009).
- ³¹B. T. Poh and Y. Y. Teh, *J. Adhes.* **90**, 802 (2014).
- ³²Y. Ohkubo, M. Shibahara, K. Ishihara, A. Nagatani, K. Endo, and K. Yamamura, *J. Adhes.* **95**, 242 (2019).
- ³³P. Kumari, C. K. Radhakrishnan, S. George, and G. Unnikrishnan, *J. Polym. Res.* **15**, 97 (2008).
- ³⁴N. Z. Noriman, H. Ismail, and A. A. Rashid, *Polym. Test.* **29**, 200 (2010).
- ³⁵T. Fukushi (to Minnesota Mining and Manufacturing Company), U.S. Patent 5,512,225, April 30, 1996.
- ³⁶K. Mori, *RUBBER CHEM. TECHNOL.* **60**, 822 (1987).
- ³⁷M. H. Chung and G. R. Hamed, *RUBBER CHEM. TECHNOL.* **62**, 367 (1989).
- ³⁸M. A. Ansarifar, J. Zhang, A. Bell, and R. J. Ellis, *Int. J. Adhes. Adhes.* **22**, 245 (2002).
- ³⁹E. Nishi and K. Masako (to Asahi Glass Company, Limited), U.S. Patent 6,655,414 B2, December 2, 2003.
- ⁴⁰M. Razavizadeh and M. Jamshidi, *Appl. Surf. Sci.* **360**, 429 (2016).
- ⁴¹G. L. McGregor and R. Winkelmayer Jr. (to W. L. Gore & Associates, Inc.), U.S. Patent 5,264,276, November 23, 1993.
- ⁴²K. Sato, T. Kato, and M. Kikuchi (to Mitsubishi Gas Chemical Company, Inc.), U.S. Patent 2017/0348941 A1, December 7, 2017.
- ⁴³G. Radonjic, *J. Appl. Polym. Sci.* **72**, 291 (1999).
- ⁴⁴S. H. Anastasiadis, I. Gancarz, and J. T. Koberstein, *Macromolecules* **22**, 1449 (1989).
- ⁴⁵J. Noolandi and K. Ming Hong, *Macromolecules* **17**, 1531 (1984).
- ⁴⁶R. Fayt, R. Jérôme, and P. Teyssié, *J. Polym. Sci. Part B Polym. Phys.* **27**, 775 (1989).
- ⁴⁷S. Al-Malaika, *Reactive Modifiers for Polymers*, Springer Science & Business Media, Berlin, 2012.
- ⁴⁸D. E. El-Nashar, *Polym. Plast. Technol. Eng.* **43**, 1425 (2004).
- ⁴⁹A. K. Bhowmick and A. N. Gent, *RUBBER CHEM. TECHNOL.* **57**, 216 (1984).
- ⁵⁰W. Smitthipong, M. Nardin, J. Schultz, and K. Suchiva, *Int. J. Adhes. Adhes.* **27**, 352 (2007).
- ⁵¹W. Smitthipong, M. Nardin, J. Schultz, and K. Suchiva, *Int. J. Adhes. Adhes.* **29**, 253 (2009).
- ⁵²W. Smitthipong, M. Nardin, J. Schultz, T. Nipithakul, and K. Suchiva, *J. Adhes. Sci. Technol.* **18**, 1449 (2004).
- ⁵³A. I. Isayev and T. Liang, *Encyclopedia of Polymer Blends*, Wiley-VCH Verlag GmbH & Co. KGaA, Weinheim, Germany, 2016.
- ⁵⁴A. A. Redhwan, A. El-Gamal, S. Khairy, and H. Hassan, *J. Thermoplast. Compos. Mater.* **29**, 92 (2016).
- ⁵⁵M. Misra, J. K. Pandey, and A. K. Mohanty, *Biocomposites: Design and Mechanical Performance*, Woodhead Publishing, Cambridge, UK, 2015.

- ⁵⁶A. F. M. Barton, *Handbook of Polymer-Liquid Interaction Parameters and Solubility Parameters*, CRC Press, Washington, DC, 1990.
- ⁵⁷S. R. Khimi and K. L. Pickering, *J. Appl. Polym. Sci.* **131**, 1 (2014).
- ⁵⁸J. R. Shelton and E. T. McDonel, *RUBBER CHEM. TECHNOL.* **33**, 342 (1960).
- ⁵⁹P. Ghosh, S. Katare, P. Patkar, J. Caruthers, and V. Venkatasubramanian, *RUBBER CHEM. TECHNOL.* **76**, 592 (2003).
- ⁶⁰N. Padhye, D. M. Parks, A. H. Slocum, and B. L. Trout, *Rev. Sci. Instrum.* **87**, 085111 (2016).
- ⁶¹J. K. Aerankavil, “Studies on Elastomer Blends with Special Reference to NBR/Butyl, NR/Butyl and NBR/EPDM Blends,” Ph.D. Thesis, Cochin University of Science and Technology, 1996.
- ⁶²M. Yaser, P. Singh, K. Pandey, V. Verma, and V. Kumar, *Ind. J. Pure Appl. Phys.* **51**, 621 (2013).

[Received May 2021, Revised March 2022]